

An Analysis of Water Infiltration in Furrow Irrigation Channels with Plants in Various Types of Soil in the Special Region of Yogyakarta Using Dual Reciprocity Boundary Element Method

Yanne Irene^{1*}, Muhammad Manaqib¹, Vina Wulandari Ramadhanty¹, Asri Ria Affriani²

¹Department of Mathematics, UIN Syarif Hidayatullah Jakarta, Indonesia

²Department of Mapping Survey and Geographic Information, Universitas Pendidikan Indonesia, Indonesia

yanne.irene@uinjkt.ac.id

ABSTRACT

Article History:

Received : 27-10-2023

Revised : 24-04-2024

Accepted : 25-04-2024

Online : 17-07-2024

Keywords:

Furrow irrigation;

Root water uptake;

Type of soil;

Drbem.



The analysis of water infiltration channels requires significant time and cost when conducted through laboratory experiments. Alternatively, mathematical modeling followed by numerical method can be employed. The mathematical model of water infiltration in furrow irrigation channels takes the form of a boundary value problem, with the Helmholtz equation serving as the governing equation. The Dual Reciprocity Boundary Element Method (DRBEM) is a numerical method derived from the Boundary Element Method (BEM), utilized for solving partial differential equations encountered in mathematical physics and engineering. This research employs DRBEM to analyze infiltration in trapezoidal irrigation channels with root-water uptake across various homogeneous soil types prevalent in agricultural lands in each District/City of the Yogyakarta Special Region Province. The results demonstrate that DRBEM provides numerical solutions for suction potential, water content, and root water absorption for each soil type. It was found that sandy soil exhibits high water content but has a low rate of root water absorption. On the other hand, clayey soil has low water content but a higher rate of root water uptake. These findings indicate that sandy soil, such as those found in Sleman District and Yogyakarta city, are less efficient in water usage when employing the furrow irrigation system, whereas clayey soil, as found in Gunung Kidul regency, is more effective.



<https://doi.org/10.31764/jtam.v8i3.19873>



This is an open access article under the **CC-BY-SA** license

A. INTRODUCTION

Agriculture is one of the sectors crucial for human sustenance, as it is a primary source of food production. Irrigation is a human endeavor aimed at distributing water to agricultural crops. One efficient method of surface irrigation is the furrow irrigation method. It is known that soil closer to the furrow contains more water compared to soil farther from the furrow. Additionally, the process of water infiltration into the soil involves changes in soil conditions and water content. This indicates that the infiltration process is not a simple matter but rather quite complex. The complexity of water infiltration in the soil makes laboratory experimentation challenging. Moreover, conducting research in a laboratory is expensive due to costly equipment and requires a substantial amount of time to obtain regular data.

One approach to understanding and addressing real-world issues is through mathematical modeling (Manaqib et al., 2019). Similarly, the issue of infiltration in irrigation channels can be modeled mathematically. The first Batu (1978) modeled the infiltration of flat-shaped irrigation channels and solved it exactly. The mathematical model for water infiltration in furrow irrigation channels takes the form of a modified Helmholtz equation in the form of a partial differential equation (PDE) with boundary conditions, or in mathematical terms, a Boundary Value Problem (BVP). Analytical solutions for this model can still be obtained when the shape of the irrigation channel is straightforward, as demonstrated by (Batu, 1978). For flat-bottomed channels. However, in practice, flat-bottomed channels are rarely used; more common shapes include trapezoidal, semicircular, and rectangular. Analytical solutions for channels with shapes other than flat are challenging to obtain. One solution approach is to use the Dual Reciprocity Boundary Element Method (DRBEM).

DRBEM is an extension of the Boundary Element Method (BEM), which is a numerical method used to solve partial differential equations encountered in mathematical physics and engineering. Examples include Laplace's equation, Helmholtz's equation, convection-diffusion equation, potential and viscous flow equations, electrostatic and electromagnetic equations, as well as linear elastostatic and elastodynamic equations (Pozrikidis, 2002). The main idea of the Boundary Element Method is to express the solution of the PDE as an integral equation on the boundary that involves the fundamental solution of the PDE. Not all PDEs have easily obtainable fundamental solutions, such as the Helmholtz equation, which is the mathematical model for water infiltration. Therefore, DRBEM was developed as an extension of BEM to solve PDEs with challenging fundamental solutions. Several studies have used DRBEM to address water infiltration issues in irrigation channels.

Azis et al. (2003) conducted a study titled "A boundary element method for steady infiltration from periodic channels," using three different channel types: flat strip, semi-circular, and rectangular, with impermeable bottom additions. This study aimed to determine the Matrix Flux Potential (MFP) values for each channel type. With the same channel length, the results indicated that the MFP values for flat strip and semi-rectangular channels were similar, while the MFP value for rectangular channels increased compared to the other two. Lobo et al. (2005) conducted a study titled "Infiltration from Irrigation Channels into Soil with Impermeable Inclusions," where they calculated the numerical MFP values for homogeneous soil using single semi-circular and dual semi-circular channels, including three different impermeable inclusions (rectangle, circular, and square). The study aimed to compare the MFP values between single and double semi-circular channels. The results showed that the MFP for double semi-circular channels was twice as high as for single semi-circular channels.

Imam Solekhdin and Keng-Cheng Ang conducted research on "A DRBEM with a predictor-corrector scheme for steady infiltration from periodic channels with root-water uptake" (Solekhdin & Ang, 2012a). This study involved root-water uptake between two channels in homogeneous soil. Using four different channel types, specifically flat, semi-circular, rectangular, and trapezoidal channels, the research aimed to compare the Matrix Flux Potential (MFP) solutions for infiltration problems with and without root-water uptake for each channel type. The results showed that using root water uptake reduced the water content values for each channel type compared to soil without root water uptake, as it was due to the water

absorption by plant roots. Another study by Imam Solekhdin and Sumardi (2017) was titled "A DRBEM for steady infiltration from periodic semi-circular channels with two different types of roots distribution" (Solekhdin & Sumardi, 2017). This study addressed infiltration in homogeneous soil with semi-circular channels while considering root-water uptake. The results showed that the two types of roots had different maximum points. Water absorption by both types of roots indicated that root A had higher maximum absorption than root B, but the daily water absorption by root A was lower than that of root B. A study conducted by Inayah et al. (2021), titled "Furrow Irrigation Infiltration in Various Soil Types Using Dual Reciprocity Boundary Element Method," analyzed infiltration in furrow irrigation channels using four different soil types without considering the plant factor. The results indicated that sandy soil had a higher water content compared to clayey soil (Inayah et al., 2021).

Daerah Istimewa Yogyakarta (DIY) (Special Region of Yogyakarta) is one of the provinces in Indonesia with an area of 3,185, 80 km² or 0.17 percent of Indonesia's area (DI Yogyakarta Central Agency, 2022). Land use in DIY is mostly for agricultural land, namely 239,160 km² or 75.07% of the area of this province. This is because 531,559 people or 28.18% of the population of DIY work as farmers. Despite its agricultural significance, DIY does not have an abundance of water, and many areas in the province experience water scarcity during the dry season. Therefore, a study focusing on water infiltration in furrow irrigation channels for different soil types in DIY would be highly valuable.

Based on the previous research above, both (Solekhdin & Ang, 2012a) and (Solekhdin & Sumardi, 2017) involved plant roots in their studies, while Inayah et al. did not. Furthermore, the variation in research conducted by (Solekhdin & Ang, 2012a) lies in the utilization of different types of channels, (Solekhdin & Sumardi, 2017) employs different types of roots, and Inayah et al. utilizes different soil types in the Banten Province. This study employs the numerical method DRBEM with predictor-corrector developed by Solekhdin & Ang (2012a) Solekhdin & Sumardi (2017) to be applied to various soil types similar to the research by Inayah et al., particularly the predominant agricultural soils in each Regency/City of DIY. The objective of this research is to determine the efficiency of furrow irrigation channel on four dominant homogenous agricultural soil types in DIY by seeking their suction potential, water content, and root water absorption values. This study is expected to provide insights into the efficiency of furrow irrigation channel employment in DIY.

B. METHODS

The mathematical model of water infiltration in furrow irrigation channels is the modified Helmholtz equation with boundary condition problems (BCP). The next step involves solving the model using DRBEM. Therefore, the solution of the Helmholtz Equation using DRBEM is explained as follows. The Helmholtz equation has a domain in R that is bounded by curve C . The two-dimensional Helmholtz equation has the following general form.

$$\frac{\partial^2 \phi(x, y)}{\partial x^2} + \frac{\partial^2 \phi(x, y)}{\partial y^2} + k^2 \phi(x, y) = g(x, y) \quad (1)$$

The boundary conditions for equation (1)are

$$\phi = f_1(x, y) \text{ for } (x, y) \in C_1 \tag{ 2}$$

$$\frac{\partial \phi}{\partial n} = f_2(x, y) \text{ for } (x, y) \in C_2 \tag{ 3}$$

The general procedure for solving the Helmholtz Equation with boundary conditions is as follows (Inayah et al., 2021).

1. Using the *reciprocal relationship* Poisson's equation to determine the *reciprocal relationship* between the solution to the Helmholtz equation ($\phi(x, y)$) that will be searched for and the fundamental solution of Laplace's equation ($\Phi(x, y; \xi, \eta)$) in the domain R .

$$\int_C \left(\Phi(x, y; \xi, \eta) \frac{\partial \phi(x, y)}{\partial n} - \phi(x, y) \frac{\partial \Phi(x, y; \xi, \eta)}{\partial n} \right) ds(x, y) = \tag{ 4}$$

$$\iint_R \Phi(x, y; \xi, \eta) (g(x, y) - k^2 \phi(x, y)) dx dy,$$

with $\Phi(x, y; \xi, \eta) = \frac{1}{4\pi} \ln((x - \xi)^2 + (y - \eta)^2)$ and $x \neq \xi, y \neq \eta$.

2. Utilizing the *reciprocal relationship* between the solution of the Helmholtz Equation and the fundamental solution of the Laplace Equation and modifying the domain to form the boundary integral equation of the Helmholtz Equation.

$$\lambda(\xi, \eta) \phi(\xi, \eta) = \int_C \left(\phi(x, y) \frac{\partial \Phi(x, y; \xi, \eta)}{\partial n} - \Phi(x, y; \xi, \eta) \frac{\partial \phi(x, y)}{\partial n} \right) ds \tag{ 5}$$

$$+ \iint_R \Phi(x, y; \xi, \eta) (g(x, y) - k^2 \phi(x, y)) dx dy$$

with

$$\lambda(\xi, \eta) = \begin{cases} 0, & \text{jika } (\xi, \eta) \notin R \cup C \\ \frac{1}{2}, & \text{jika } (\xi, \eta) \text{ pada bagian smooth } C \\ 1, & \text{jika } (\xi, \eta) \in R \end{cases}$$

3. Approaching the integral domain of the Helmholtz Equation boundary integral equation (5) by using a linear combination of certain radial basis functions centered at the collocation points $(a^{(m)}, b^{(m)})$, $m = 1, 2, \dots, M$.

$$\iint_R \Phi(x, y; \xi, \eta)(g(x, y) - k^2 \phi(x, y)) dx dy$$

$$= \sum_{j=1}^M \left[\sum_{m=1}^M \omega(a^{(j)}, b^{(j)}; a^{(m)}, b^{(m)}) \Psi(\xi, \eta; a^{(m)}, b^{(m)}) \right] \quad (6)$$

$$[g(a^{(j)}, b^{(j)}) - k^2 \phi(a^{(j)}, b^{(j)})]$$

with

$$\Psi(\xi, \eta; a^{(m)}, b^{(m)}) = \lambda(\xi, \eta) \chi(\xi, \eta; a^{(m)}, b^{(m)}) +$$

$$\int_C \left(\Phi(x, y; \xi, \eta) \frac{\partial \chi(x, y; a^{(m)}, b^{(m)})}{\partial n} - \chi(x, y; a^{(m)}, b^{(m)}) \frac{\partial \Phi(x, y; \xi, \eta)}{\partial n} \right) ds,$$

$$\chi(\xi, \eta; a^{(m)}, b^{(m)})$$

$$= \frac{1}{4} r^2(x, y; a^{(m)}, b^{(m)}) + \frac{1}{16} r^4(x, y; a^{(m)}, b^{(m)})$$

$$+ \frac{1}{25} r^5(x, y; a^{(m)}, b^{(m)}).$$

4. Substitute Equation (6) into (5) to obtain the boundary integral equation form of the Helmholtz Equation in the line integral form.

$$\lambda(\xi, \eta) \phi(\xi, \eta) = \sum_{j=1}^M \left[\sum_{m=1}^M \omega(a^{(j)}, b^{(j)}; a^{(m)}, b^{(m)}) \Psi(\xi, \eta; a^{(m)}, b^{(m)}) \right]$$

$$[g(a^{(j)}, b^{(j)}) - k^2 \phi(a^{(j)}, b^{(j)})] \quad (6)$$

$$+ \int_C \left(\Phi(x, y) \frac{\partial \Phi(x, y; \xi, \eta)}{\partial n} - \Phi(x, y; \xi, \eta) \frac{\partial \phi(x, y)}{\partial n} \right) ds$$

for $(\xi, \eta) \in R \cup C$

5. Substitute the collocation points $(\bar{x}^{(j)}, \bar{y}^{(j)})$, $j = 1, 2, \dots, N + L$ with N is the number of collocation points in the interior domain and L is the number of collocation points on the boundary domain, to obtain a system of linear equations with the variables to be determined $\bar{\phi}^{(k)}$ and $\bar{p}^{(k)}$.

$$\lambda(a, b) \phi(a, b) = \sum_{j=1}^{N+L} \mu^{(j)} [g(\bar{x}^{(j)}, \bar{y}^{(j)}) - k^2 \bar{\phi}^{(j)}]$$

$$+ \sum_{k=1}^N [\bar{\phi}^{(k)} F_2^{(k)}(a, b) - \bar{p}^{(k)} F_1^{(k)}(a, b)] \quad (7)$$

with

$$\lambda(a, b) = \begin{cases} \frac{1}{2}, & \text{jika } (a, b) \text{ pada bagian smooth } C \\ 1, & \text{jika } (a, b) \in R \end{cases}$$

$$F_1^{(k)}(a, b) = \frac{1}{4\pi} \int_{C^{(k)}} \ln((x - a)^2 + (y - b)^2) ds$$

$$F_2^{(k)}(a, b) = \frac{1}{4\pi} \int_{C^{(k)}} \frac{\partial}{\partial n} [\ln((x - a)^2 + (y - b)^2)] ds$$

6. Solve the system by substituting the solution Equation (8) into the boundary integral equation to obtain an equation that is used to evaluate the Helmholtz Equation at each point in the domain.

$$\begin{aligned} \lambda(a, b)\phi(a, b) &= \sum_{j=1}^{N+L} \mu^{(j)} [g(\bar{x}^{(j)}, \bar{y}^{(j)}) - k^2 \bar{\phi}^{(j)}] \\ &+ \sum_{k=1}^N [\bar{\phi}^{(k)} F_2^{(k)}(a, b) - \bar{p}^{(k)} F_1^{(k)}(a, b)] \end{aligned} \tag{8}$$

for $(a, b) \in C \cup R$.

Moreover, the DRBEM can be integrated into computer programming languages, which involves three main phases: Pre-Processing, Processing, and Post-Processing. During the Pre-Processing phase, essential components such as interior and exterior collocation points, domain discretization, and boundary conditions are prepared. The boundaries are discretized using 200-line segments and 625 interior points. In the Processing phase, the DRBEM method is applied. Finally, in the Post-Processing phase, a specified number of points within the domain are evaluated as required.

C. RESULTS AND DISCUSSION

1. Problem Formulation

Special Region of Yogyakarta is one of the provinces in Indonesia which is located between 7.33–8.12 South Latitude and 110.00 –110.50 East Longitude, recorded as having an area of 3,185,80 km² or 0.17 percent of the area of Indonesia (DI Yogyakarta Central Agency, 2015). Land use in Special Region of Yogyakarta is mostly for agricultural land, about 239,160 km² or 75.07% of the area of this province, as seen in Figure 1.

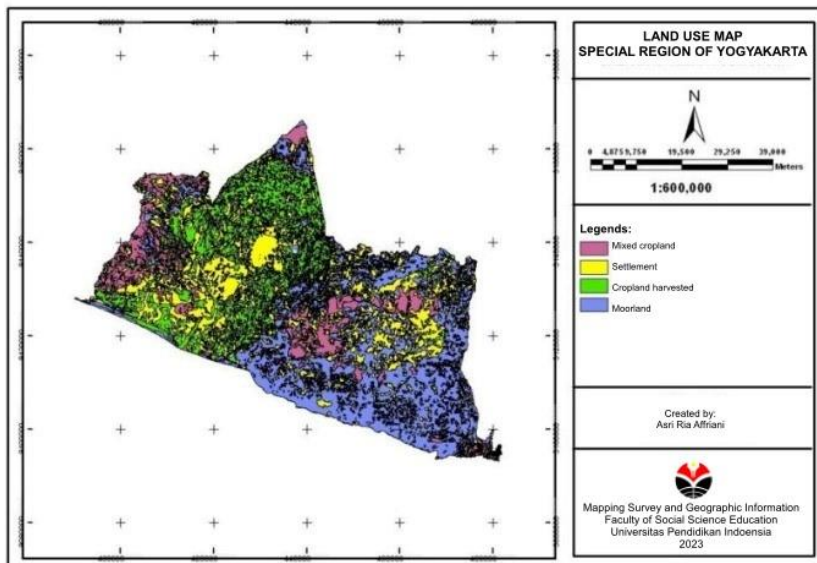


Figure 1. Land Use Map of the Special Region of Yogyakarta

Soil types based on order names in DI Yogyakarta are Alluvial, Grumusol, Kambisol, Lathosol, Mediteran, and Regosol, the distribution of which can be seen in Figure 2 Map of Soil Types of the Special Region of Yogyakarta.

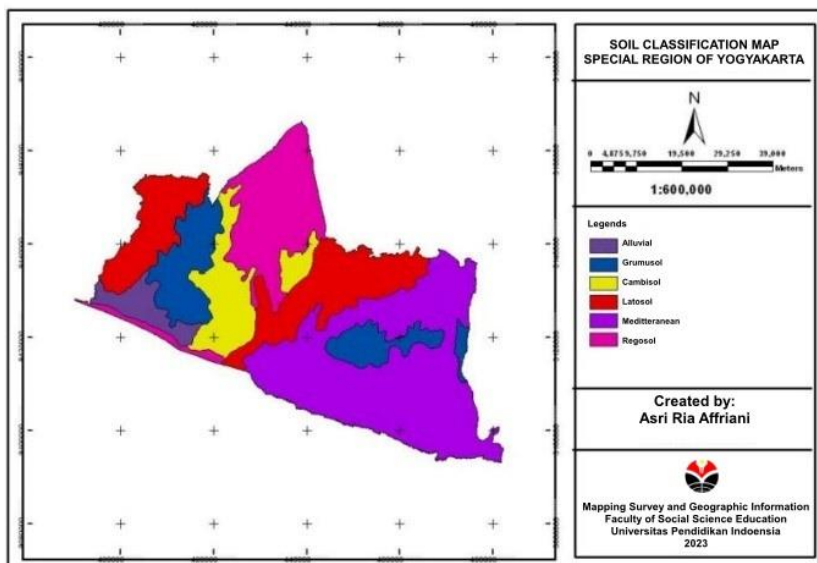


Figure 2. Soil Type Map of the Special Region of Yogyakarta.

The Land Use Map of the Special Region of Yogyakarta and the Soil Type Map of the Special Region of Yogyakarta can be combined using ArcGis software, to obtain the Soil Type Map of Agricultural Land of the Special Region of Yogyakarta Figure 3

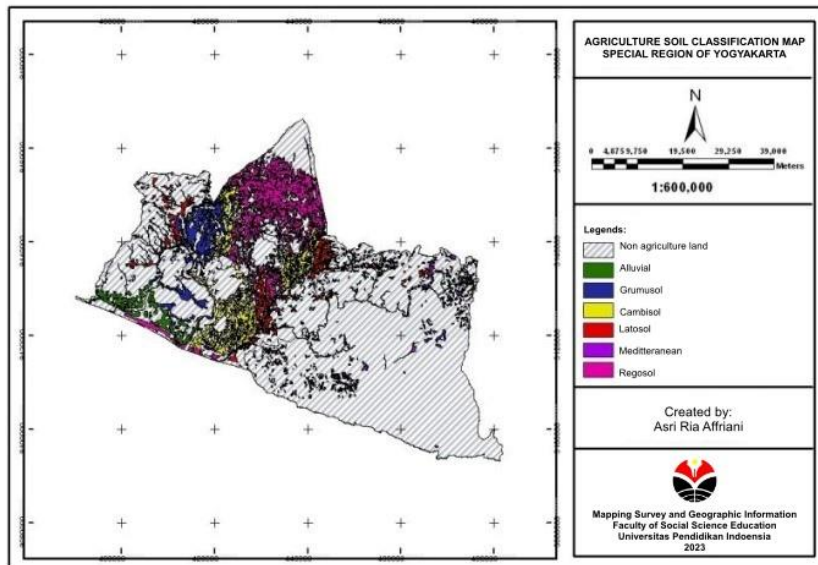


Figure 3. Soil Type Map of Agricultural Land in the Special Region of Yogyakarta

Based on Figure 3 and using ArcGis software, the area of agricultural land types for each district/city of DI Yogyakarta can be obtained. More details can be seen in Table 1 below.

Table 1. Types of Soil in Districts/Cities DI Yogyakarta

Type of soil	Area (ha)				
	Kulon Progo	Sleman	Yogyakarta	Bantul	Gunung Kidul
Alluvial	44,067.84	0	0	159.88	0
Grumusol	4,921.04	4,379.98	0	613.17	570.06
Latosol	3,398.94	1,600.86	0	4,336.85	2,004.84
Regosol	971.88	19,844.08	335.39	3,147.30	0
Cambisole	141.35	3,844.68	0.11	9,669.22	0
Mediterranean	0	0	0	78.14	4,402.82

Based on Table 1, it can be seen that the dominant land order types in each district/city of the Special Region of Yogyakarta are Kulon Progo Regency has Alluvial, Sleman Regency has Regosol, Bantul Regency has Kambisol, Gunung Kidul Regency has Mediteran, and Yogyakarta City has Regosol. Furthermore, based on the (Java Ecoregion Management Center, 2015) and (Handayanto, 1987), the soil structure of the soil orders in Yogyakarta can be determined. Below is the soil structure for the dominant land order types in each district/city of DI Yogyakarta.

Table 2. Soil Structure.

No	Regency/City	Type of soil	Soil Structure
1	Kulon Progo	Alluvial	<i>Silty Clay Loam – Silty Clay</i>
2	Sleman and Yogyakarta	Regosol	<i>Loamy Sand – Sand</i>
3	Bantul	Cambisole	<i>Sandy Loam</i>
4	Gunung Kidul	Mediterranean	<i>Loam - Clay</i>

Different parameter values α and K_0 are obtained from (Amoozegar-Fard et al., 1984) and the values of θ_r , θ_s , and n respectively as residual, saturated, and potential water content values obtained from the list of values in (Warrick, 2002).

Table 3. Parameters for each type of soil.

Type of soil	$\alpha(\text{cm}^{-1})$	$K_0(\text{cm}\backslash\text{s})$	θ_r	θ_s	n
Lakish Clay	1.38×10^{-2}	8.1×10^{-5}	0.068	0.38	1.09
Plainfield Sand	2.62×10^{-2}	0.03	0.045	0.38	1.09
Sheluhot Silty Clay	7.26×10^{-3}	1.44×10^{-6}	0.07	0.36	1.09
Yolo Fine Sandy Loam	2.5×10^{-2}	4.07×10^{-5}	0.065	0.41	1.89

2. Mathematical Model of Infiltration in Furrow Irrigation Channels with root water uptake

The surface of irrigation channel system uses a trapezoidal shape, which is a channel cross-sectional shape that is commonly applied in Indonesia. Using the trapezoidal cross-sectional channel, several assumptions are given as follows (Solekhudin & Zulijanto, 2017) .

- a. Irrigation channels have the same channel width and a sufficient length; hence the length of the irrigation channel is ignored in this model.
- b. The cross-sectional length of the trapezoidal irrigation channel surface is $2L$.
- c. The midpoint between two adjacent channels has a distance of $2(L + D)$.
- d. The cross section of the irrigation channel is always filled with water.
- e. Other irrigation channels have negligible influence.
- f. The rate of water infiltration / the amount of *flux* (flow) entering the channel surface is constant at v_0 .
- g. The incoming water flow only comes from the channel.

Using Cartesian coordinates, the coordinates used for furrow irrigation channels are $OXYZ$ with the center point O and the depth of the channel OZ which has a positive value. Having the assumption that the width of the channel and the distance between the channels are the same size, then the cross-sectional shape of the channel along its length OY is assumed to have not changed and is symmetrical for $X = \pm k(L + D)$, $k = 0, \pm 1, \pm 2, \pm 3, \dots$. The state of the flow pattern is considered to have two dimensions (Solekhudin & Ang, 2012b) . Because this research includes root water absorption, it is illustrated that there is a plant between two adjacent channels with a depth Z_m and width $2X_m$ and the distance between the two plants is $2(L + D)$, as shown in Figure 4.

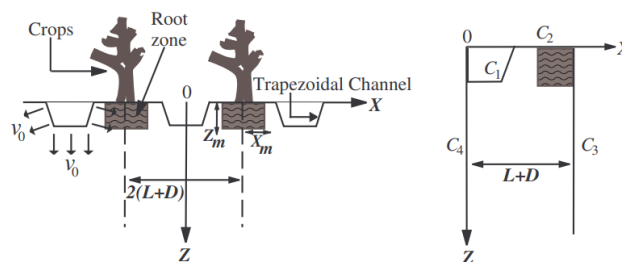


Figure 4. The geometry of two-dimensional trapezoidal irrigation channels (Solekhudin & Ang, 2012b) .

Through the illustration in Figure 4 and based on the symmetric nature of the model, the analysis required is sufficient on $0 \leq X \leq L + D$ and $Z \geq 0$ with the domain $0 \leq X \leq L + D, Z \geq 0$ as a semi-infinite region, for example R . This problem involves a type of plant root which has several parameters obtained from (Vrugt et al., 2001). The selected root type has $Z^* = 0,2 \text{ m}$, $X^* = 0,25 \text{ m}$, $p_z = 5,00$, and $p_x = 2,00$. Each parameter has an explanation of where it is Z^* and X^* shows the coordinates of the location of the root in the root zone. In Z^* and X^* , the center point $(0,0)$ shows the location of the plant, where this location is farthest from the channel in the root zone. The downward X^* axis and the Z^* leftward axis have positive values. Meanwhile p_z and p_x are parameters of plant roots.

To apply this method, the width of half the channel and the width of half the ground surface are chosen, namely $L = D = 50 \text{ cm}$. The width of half the root zone is selected $X_m = 50 \text{ cm}$ and the depth of the root zone $Z_m = 100 \text{ cm}$. Meanwhile, the potential for transpiration $T_{pot} = 4 \text{ cm/day}$ (Solekhudin & Sumardi, 2017). The general equation used to find solutions in pivoted media is the Richard equation (Assouline, 2013). The equation for setting the infiltration problem using *root water uptake* using the Richard equation is given as follows (Solekhudin & Ang, 2012a).

$$\frac{\partial}{\partial X} \left(K \frac{\partial \psi}{\partial X} \right) + \frac{\partial}{\partial Z} \left(K \frac{\partial \psi}{\partial Z} \right) - \frac{\partial K}{\partial Z} = S(X, Z, \psi) \tag{9}$$

where K is hydraulic conductivity, ψ is *suction potential*, and S is a function for *root water uptake* with the following equation (Zahroh & Solekhudin, 2022).

$$S(X, Z, \psi) = \gamma(\psi) \frac{L_t \beta(X, Z) T_{pot}}{\int_0^{Z_m} \int_{L+D-X_m}^{L+D} \beta(X, Z) dX dZ} \tag{10}$$

with γ is a response function of water pressure and salinity, L_t is the width of the soil surface related to transpiration, $\beta(X, Z)$ is a two-dimensional spatial distribution of roots, and T_{pot} is the potential for transpiration

$$\beta(X, Z) = \left(1 - \frac{L + D - X}{X_m} \right) \left(1 - \frac{Z}{Z_m} \right) e^{-\left(\frac{p_z}{Z_m} |Z^* - Z| + \frac{p_x}{X_m} |X^* - X| \right)} \tag{11}$$

for $L + D - X_m \leq X \leq L + D, 0 \leq Z \leq Z_m$,

where L is the width of half the channel, D is the width of the ground surface outside the channel, p_z, p_x, X^* , and Z^* is an empirical parameter, and X_m is the width of the root zone, and Z_m is the depth of the root zone. Richard's equation (9) will be transformed into the Helmholtz equation (Stone, 1978). The steps are as follows.

a. Kirchoff Transformations

$$\theta = \int_{-\infty}^{\infty} K ds \quad (12)$$

b. Exponential model of hydraulic conductivity

$$K = K_s e^{\alpha\psi}, \quad \alpha > 0 \quad (13)$$

c. Transformation into dimensionless variables

$$x = \frac{\alpha}{2} X; \quad z = \frac{\alpha}{2} Z; \quad \Phi = \frac{\pi\theta}{v_0 L}; \quad u = \frac{2\pi}{v_0 \alpha L} U; \quad v = \frac{2\pi}{v_0 \alpha L} V; \quad f = \frac{2\pi}{v_0 \alpha L} F \quad (14)$$

so, it is obtained

$$\frac{\partial^2 \phi}{\partial^2 x} + \frac{\partial^2 \phi}{\partial^2 z} - \phi = \gamma^*(\phi) s^*(x, z) \quad (15)$$

is a modified Helmholtz equation that includes *root-water uptake*. Based on the above assumptions, the boundary conditions can be formulated as follows.

$$\frac{\partial \phi}{\partial n} = \frac{2\pi}{\alpha L} e^{-z} + \phi n_2, \text{ pada permukaan saluran} \quad (16)$$

$$\frac{\partial \phi}{\partial n} = -\phi, \text{ untuk } \frac{\alpha L}{\pi} \leq x \leq b, \text{ dan } z = 0 \quad (17)$$

$$\frac{\partial \phi}{\partial n} = 0, \text{ untuk } x = b \text{ dan } z \geq 0 \quad (18)$$

$$\frac{\partial \phi}{\partial n} = 0, \text{ untuk } x = 0 \text{ dan } z \geq \frac{3\alpha L}{4\pi} \quad (19)$$

$$\frac{\partial \phi}{\partial n} = -\phi, \text{ untuk } 0 \leq x \leq b \text{ dan } z = \infty \quad (20)$$

To solve using DRBEM, the domain R must be closed and finite, whereas in the model, the domain R is a semi-infinite domain. So, domain restrictions are required by assuming $z = c$, with c is a positive real number. So, equation (20) is changed to:

$$\frac{\partial \phi}{\partial n} = -\phi, \text{ untuk } 0 \leq x \leq b \text{ dan } z = c \quad (21)$$

The line segment is defined C_1, C_2, C_3, C_4, C_5 as follows.

$$C_1: \text{permukaan saluran} \quad (22)$$

$$C_2: \frac{\alpha L}{\pi} \leq x \leq b, \text{ dan } z = 0 \tag{23}$$

$$C_3: x = b \text{ dan } 0 \leq z \leq c \tag{24}$$

$$C_4: x = 0 \text{ dan } \frac{3\alpha L}{4\pi} \leq z \leq c \tag{25}$$

$$C_5: 0 \leq x \leq b \text{ dan } z = c \tag{26}$$

The mathematical model of water infiltration in furrow irrigation channel with root water uptake can be systematically represented in Figure 5.

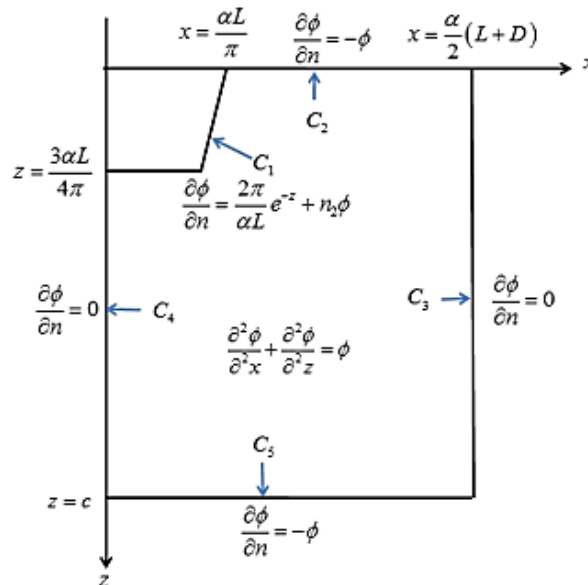


Figure 6. The mathematical model of water infiltration in furrow irrigation channel with root water uptake.

3. Solution Using Dual Reciprocity Boundary Element Method (DRBEM)

To solve the problem of infiltration of irrigation channels using DRBEM with a predictor-corrector scheme, it was carried out using the Matlab program. DRBEM was implemented into the Matlab program, and used to solve the problem of infiltration of furrow irrigation channels with *root water uptake* in four types of homogeneous soil afterwards. Each type of soil has values $\alpha, K_0, \theta_r, \theta_s,$ and $n,$ so the implementation of this program adjusts the values of these parameters which refer to Table 3. Apart from adjusting the parameter values, the number of line segments in the domain discretization with a value was chosen $N = 200$ because according to (Solekhudin & Ang, 2012b) this value provides good accuracy in the results of the numerical approach, while the value M chosen $M = 625$. Each type of soil was evaluated for the *suction potential value* (ψ) and *water content* (θ) at several points along the line, namely at $X = 10, X = 30, X = 50, X = 70,$ and $X = 90$ for $0 \leq Z \leq 200$ cm. The value of ψ and θ for each land is depicted on a graph that can display the relationship between ψ and θ for each type of land, as shown in Figure 6.

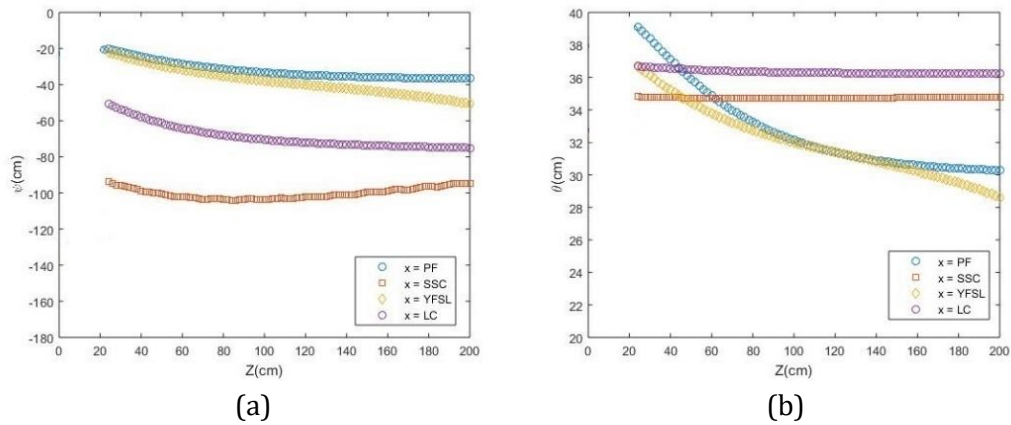


Figure 7. Suction Potential and Water Content in Four Types of Soil for $X = 10$.

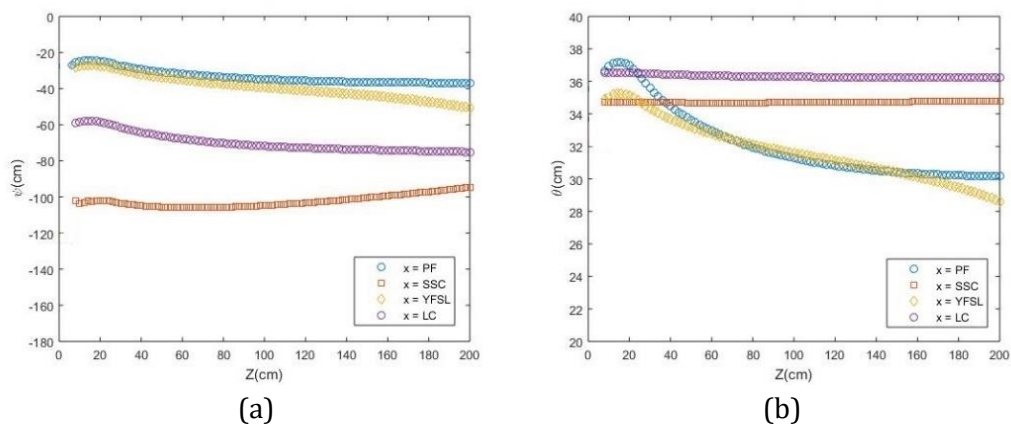


Figure 8. Suction Potential and Water Content in Four Types of Soil for $X = 30$.

Figure 6 and Figure 7 are graphs of the values ψ and θ of the four types of soil below the channel, namely at $X = 10$ and $X = 30$, with $0 \leq Z \leq 200$ cm. Evaluation along this line shows that the value pattern ψ and θ of three types of soil (*Lakish Clay*, *Plainfield Sand*, and *Yolo Fine Sandy Loam*) decreases while increasing the depth towards the point of convergence, while one type of soil (*Sheluhot Silty Clay*) increases along with increasing the depth. However, the shape of the given curve varies depending on the type of soil. Based on Figure 6(b) and Figure 7(b), it is shown that the water content in each type of soil also has a different pattern and curve shape. However, this is directly proportional to the value ψ . This indicates that the water content is higher at shallow depths at the position below the channel. The large value θ at shallow depth is in accordance with the assumption that water only enters from the channel and then spreads into the soil below the channel.

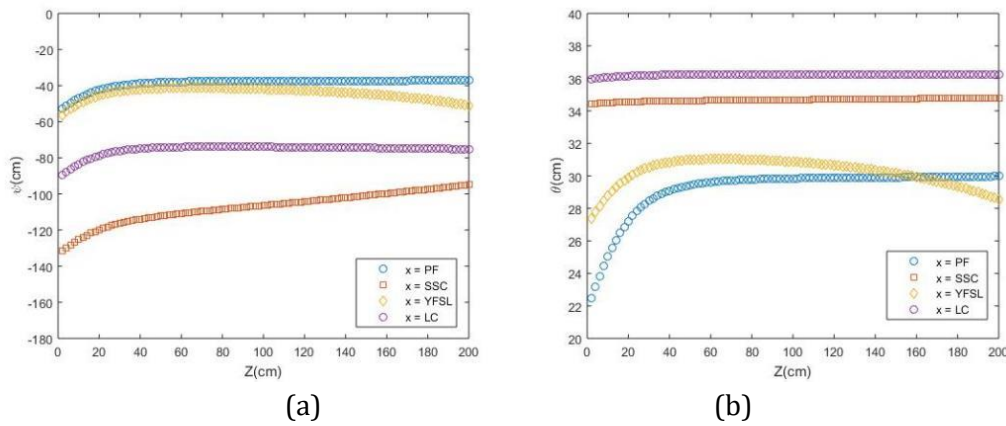


Figure 9. Suction Potential and Water Content in Four Types of Soil for $X = 50$ cm.

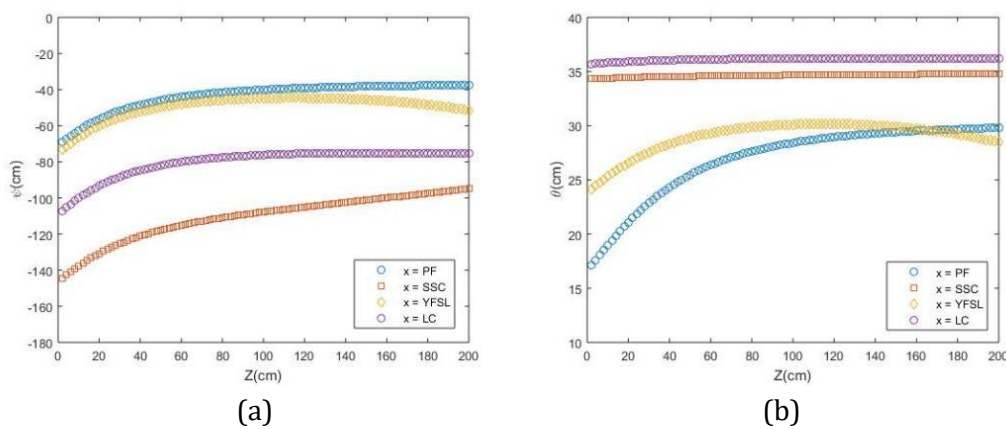


Figure 10. Suction Potential and Water Content in Four Types of Soil for $X = 70$ cm.

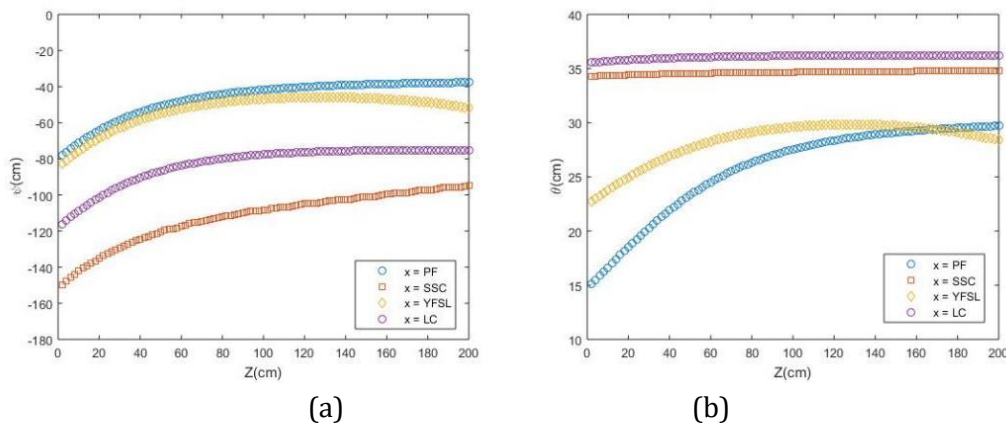


Figure 11. Suction Potential and Water Content in Four Types of Soil for $X = 90$ cm.

Next, to evaluate along lines other than at positions below the channel, select $X = 50$ cm, $X = 70$ cm, and $X = 90$ cm, for $0 \leq Z \leq 200$ cm. Based on the graphs in Figure 8, Figure 9, and Figure 10, it is known that there is an increase in the value of ψ and θ for each type of soil as the depth of the soil increases towards the point of convergence. Thus, it shows the *suction potential value* which is directly proportional to *the water content value*. These results corroborate the conclusions drawn in the evaluation for the lines below the channel. Apart from that, the value θ also increases with increasing depth, indicating that this is in accordance with

the assumption that there is no incoming water flow other than from the channel, because at a lower position, the water content of each soil is also low.

Based on the graph in Figure 9(a) – Figure 11(a), it shows that in the same position the order of soil types with suction potential (ψ) values from highest to lowest is Plainfield Sand, Yolo Fine Sandy Loam, Lakish Clay, and Sheluhot Silty Clay. Based on **Error! Reference source not found.**, if it is related to the value α for each type of soil, it can be concluded that the lower the value of α a type of soil, the lower the suction potential value. So, it can be concluded from the texture of a type of soil, where soil with a fine texture has a lower suction potential value compared to soil with a coarse texture such as sandy soil.

Based on the graph in Figure 9(b) – Figure 11(b), which shows the pattern of *water content* in each type of soil, the order of values θ from the highest in the same position is *Lakish Clay, Sheluhot Silty Clay, Yolo Fine Sandy Loam, and Plainfield Sand*. This shows that clay soil, *Lakish Clay* and *Sheluhot Silty Clay*, have a high-water content value and a constant graph compared to sandy soil, so it is indicated that clay soil can hold water so that it does not easily absorb it and run out downwards. Meanwhile, *Plainfield Sand* and *Yolo Fine Sandy Loam* soils have high absorption capacity so that the water content in them decreases as depth increases. Because the value θ indicates the water content of each type of soil, it can be concluded that soil with a clay and fine texture has a higher water content than sandy soil.

To determine the distribution pattern of *suction potential* and *water content* values in the domain R for each type of soil, the values of ψ and θ then evaluated using a *surface plot*. The domain used is a trapezoidal channel with width 100 cm and depth 200 cm for the four types of soil. To make it easier to evaluate, the graph presented uses color at certain points in the domain to show the *suction potential* or *water content* value which is adjusted to the legend on the right of the graph.

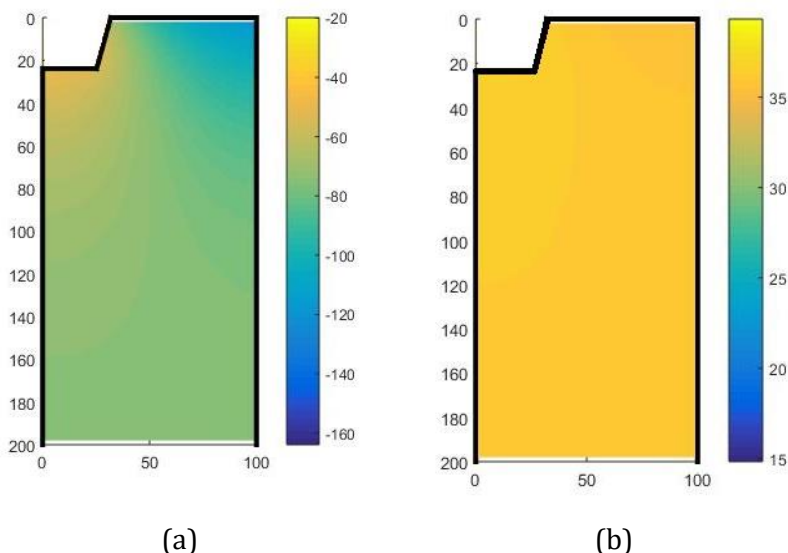
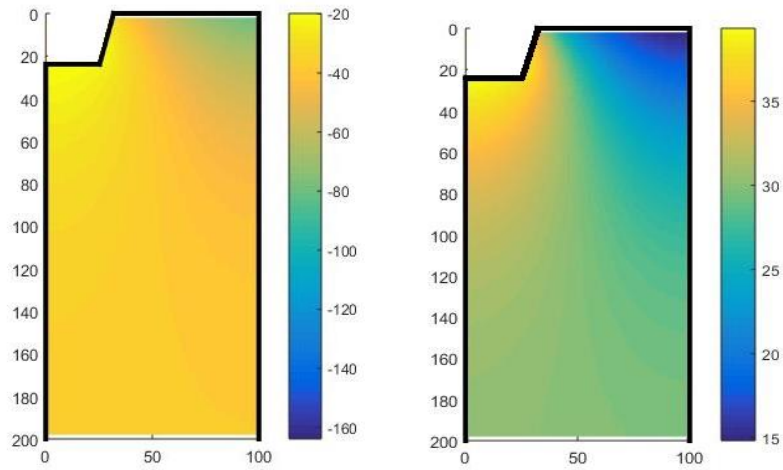
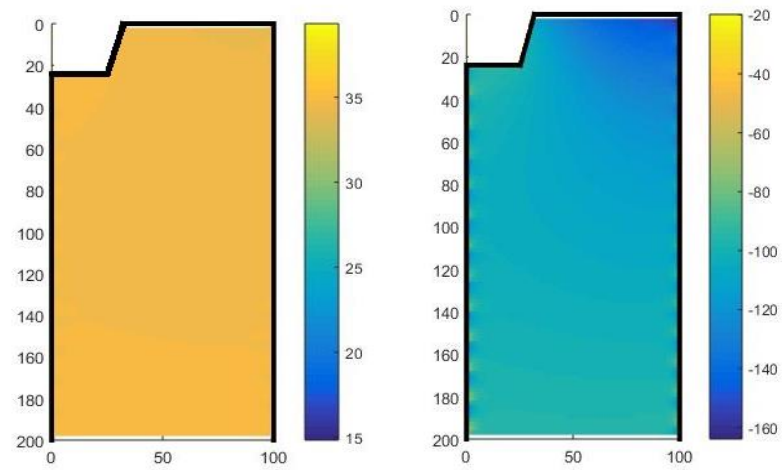


Figure 11. Suction Potential and Water Content in Lakish Clay soil.
 (a) Suction Potential (cm); and (b) Water Content (%)



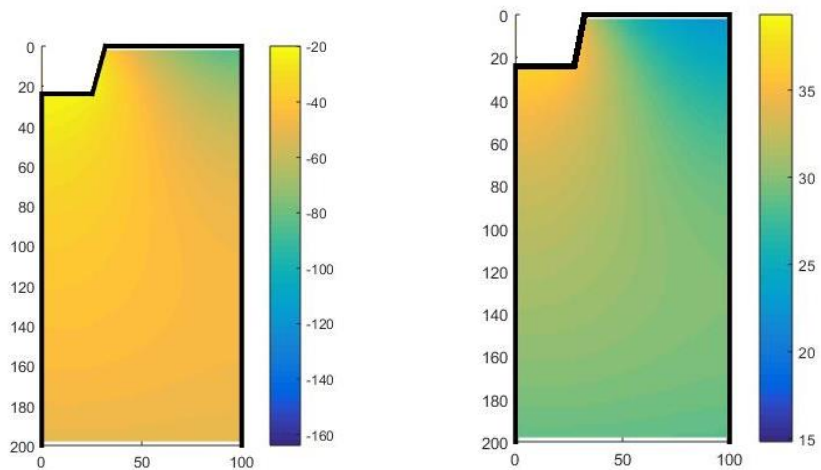
(a) Suction Potential (cm) (b) Water Content (%)

Figure 12. Suction Potential and Water Content in Plainfield Sand soil.



(a) Suction Potential (cm) (b) Water Content (%)

Figure 13. Suction Potential and Water Content in Sheluhot Silty Clay soil.



(a) Suction Potential (cm) (b) Water Content (%)

Figure 14. Suction Potential and Water Content on Yolo Fine Sandy Loam.

Based on Figure(a) – Figure 14(a), it can be concluded that the highest suction potential value is located directly below the channel, while other surfaces have lower values. The lowest value is shown on the ground surface which is farthest from the channel. In the upper soil layer of the domain, we can see quite significant differences in suction potential values. It is shown that the farther away from the channel, the lower the suction potential value. Meanwhile, the underground layer has a suction potential value that is almost constant regardless of how far it is from the center of the channel. It can be seen that this distribution pattern is the same for all types of soil.

Figure(b) – Figure 14(b) shows the pattern of water content in the domain *R* for each soil type. Based on the graph above, the water content value directly below the channel has the highest value, while the lowest value is located on the surface at the farthest distance from the channel. Having the same pattern as the distribution pattern of suction potential values previously explained, the water content values for all types of soil have differences in the upper and lower layers of soil. In the upper layer, it can be concluded that the water content value decreases as the distance of the ground surface from the center of the channel increases. Meanwhile, for the bottom layer, no matter how far the soil surface is from the center of the channel, the water content in the soil tends to be constant. Based on the picture, it can be seen that *the Sheluhot Silty Clay soil* contains the most water, followed by the *Lakish Clay soil*. These two types of soil have a dominant yellow color on *the surface plot* domain, which indicates a fairly high-water content value. Meanwhile, the *Plainfield Sand* and *Yolo Fine Sandy Loam* soil types have brighter *surface plot colors and are dominated by greenish*. This shows that the water content in these two types of soil is lower. Systematically, the minimum and maximum values of *suction potential* and *water content* for the four types of soil are attached to Tables follows.

Table 4. Minimum and maximum *suction potential* and *water content* values for the four types of soil.

No	Regency/City	Type of soil	Suction Potential (cm)		Water Content (%)	
			Min	Max	Min	Max
1	Gunung Kidul	<i>Lakish Clay</i>	-117.3560	-25.4101	35.5510	36.7081
2	Sleman and Yogyakarta	<i>Plainfield Sand</i>	-79.5743	-19.8292	14.8238	39.3370
3	Kulon Progo	<i>Sheluhot Silty Clay</i>	-163.9195	-25.4101	34.1632	36
4	Bantul	<i>Yolo Fine Sandy Loam</i>	-84.0855	-21.8657	22.5599	36.7791

Based on Table can strengthen the conclusions based on Figure– Figure 14, which states that each type of soil has a different level of absorption (suction potential) and water content. The type of soil that contains a lot of water is *Lakish Clay*, followed by *Sheluhot Silty Clay*, *Yolo Fine Sandy Loam*, and *Plainfield Sand* in order. This shows that clay-textured soil contains more water because it can hold water better than coarse-textured soil (sand). Next, to see the pattern of water absorption in the roots of each type of soil in the domain, a surface plot was formed with 200 *cm* the following depth and width 100 *cm*.

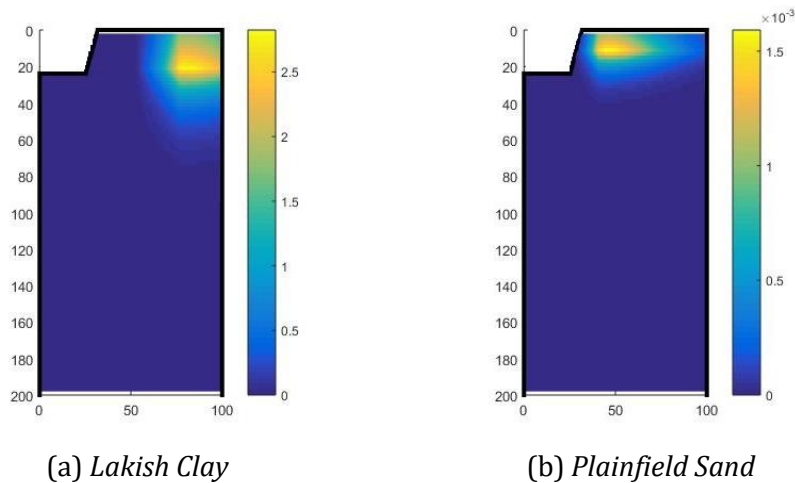


Figure 15. Root water uptake in Lakish Clay and Plainfield Sand Soils.

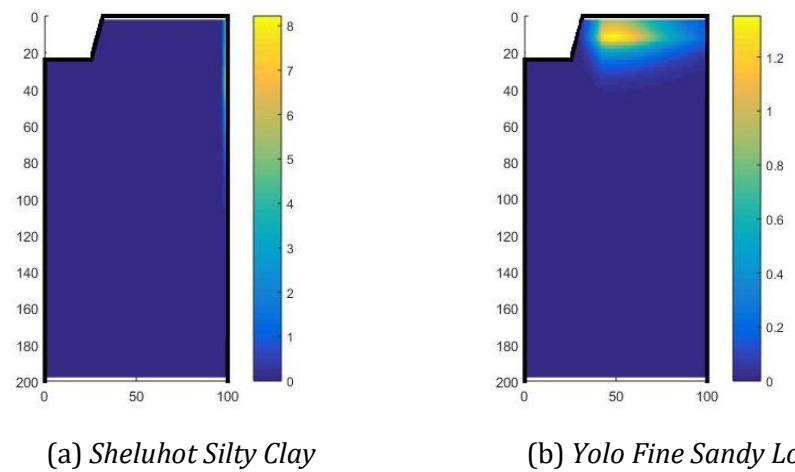


Figure 16. Root Water Uptake in Sheluhot Silty Clay and Yolo Fine Sandy Loam Soils.

Based on Figure 15 and Figure 16 shows that water absorption by the roots of the four types of soil studied has a different distribution and maximum point of water absorption. The total amount of water absorbed by the roots of each type of soil per day is shown in the following Table 5.

Table 5. Total Water Absorption Value from Each Soil.

No.	Type of soil	Total Absorption (cm^2/day)
1	Lakish Clay	177.6343
2	Plainfield Sand	91.7788
3	Sheluhot Silty Clay	409.4246
4	Yolo Fine Sandy Loam	100.0670

Based on the table above, it can be seen that the total amount of water absorbed in each type of soil in this study is significantly different, respectively 177.6343 cm^2/day for Lakish Clay soil, 91.7788 cm^2/day for Sand soil, 409.4246 cm^2/day for Silty Clay soil, and 100.0670 cm^2/day for Yolo Fine Sandy Loam soil. This shows that the sequence from the highest total daily absorption is *Sheluhot Silty Clay*, *Lakish Clay*, *Yolo Fine Sandy Loam*, and *Plainfield Sand*. Thus, plants absorb more water from fine-textured soil such as clay compared to sandy soil.

D. CONCLUSION AND SUGGESTIONS

The numerical solution for the infiltration problem of furrow irrigation in trapezoidal channels with root water uptake in various types of homogeneous soil found in the District/City of Special Region of Yogyakarta (DIY) can be achieved through the application of the Dual Reciprocity Boundary Element Method (DRBEM). This method is utilized to solve a Boundary Condition Problem (BCP) formulated with the modified Helmholtz equation as the governing equation, and mixed boundary conditions (Robin) are applied using a predictor-corrector scheme.

It was found that the dominant soil in agricultural land in Kulon Progo regency is alluvial soil, corresponding to the soil structure of Sheluhot Silty Clay. In Sleman regency and Yogyakarta city, regosol soil corresponds to the soil structure of Plainfield Sand. In Bantul regency, Yolo Fine Sandy Loam soil corresponds to the soil structure. In Gunung Kidul regency, Lakish Clay soil corresponds to the soil structure.

The study identified the sequence of highest water content around the channel as follows: Plainfield Sand, Yolo Fine Sandy Loam, Lakish Clay, and Sheluhot Silty Clay, in contrast to the sequence of root-water uptake, which is as follows: Sheluhot Silty Clay, Lakish Clay, Yolo Fine Sandy Loam, and Plainfield Sand. Therefore, it can be concluded that sandy soil exhibits high water content but has a low rate of root water absorption. On the other hand, clayey soil has low water content but a higher rate of root water uptake. These findings indicate that sandy soil, such as those found in Sleman District and Yogyakarta city, are less efficient in water usage when employing the furrow irrigation system, whereas clayey soil, as found in Gunung Kidul regency, is more effective.

ACKNOWLEDGEMENT

The authors thank to the Center of Research and Publication of UIN Syarif Hidayatullah Jakarta for providing financial support for this research with the contract number UN.01/KPA/1165/2023.

REFERENCES

- Agency, D. Y. C. (2015). *Daerah Istimewa Yogyakarta dalam Angka 2015*. <https://yogyakarta.bps.go.id/publication/2015/11/16/a5900334e7d45e855906c4e7/daerah-istimewa-yogyakarta-dalam-angka-2015.html>
- Agency, D. Y. C. (2022). *Kota Yogyakarta dalam Angka 2022*. <https://yogyakarta.bps.go.id/publication/2022/02/25/05661ba4fe09161192c3fc42/provinsi-daerah-istimewa-yogyakarta-dalam-angka-2022.html>
- Amoozegar-Fard, A., Warrick, A. W., & Lomen, D. O. (1984). Design Nomographs for Trickle Irrigation Systems. *Journal of Irrigation and Drainage Engineering*, 110(2), 107–120. [https://doi.org/10.1061/\(asce\)0733-9437\(1984\)110:2\(107\)](https://doi.org/10.1061/(asce)0733-9437(1984)110:2(107))
- Assouline, S. (2013). Infiltration into soils: Conceptual approaches and solutions. *Water Resources Research*, 49, 1755–1772. <https://doi.org/10.1002/wrcr.20155>
- Azis, M. I., L.Clements, D., & Lobo, M. (2003). A boundary element method for steady infiltration from periodic channels. *ANZIAM Journal*, 44(E), C61-C78. <https://doi.org/10.21914/anziamej.v44i0.672>
- Batu, V. (1978). Steady Infiltration from Single and Periodic Strip Sources. *Soil Science Society of America Journal*, 42.
- Handayanto, E. (1987). *Dasar-Dasar Ganesa dan Klasifikasi Tanah*. Universitas Brawijaya.
- Inayah, N., Manaqib, M., & Majid, W. N. (2021). Furrow irrigation infiltration in various soil types using dual reciprocity boundary element method. *AIP Conference Proceedings*, 2329(February).

<https://doi.org/10.1063/5.0042682>

- Katsikadelis, J. T. (2002). Boundary Elements: Theory and Applications. In *Elsevier*.
<https://doi.org/10.1201/b14924-7>
- Lobo, M., Clements, D. L., & Widana, N. (2005). Infiltration from irrigation channels into soil with impermeable inclusions. *ANZIAM Journal*, 46(E). <https://doi.org/10.21914/anziamj.v46i0.1006>
- Manaqib, M., Fauziah, I., & Mujiyanti, M. (2019). Mathematical Model for Mers-CoV Disease Transmission with Medical Mask Usage and Vaccination. *InPrime: Indonesian Journal of Pure and Applied Mathematics*, 1(2), 97–109. <https://doi.org/10.15408/inprime.v1i2.13553>
- Pozrikidis, C. (2002). A Practical Guide to Boundary Element Methods with The Software Library BEMLIB. In *International Journal of Solids and Structures* (Vol. 40, Issue 11). A CRC Press Company.
- Progo, D. (2015). *Pusat Pengelolaan Ekoregion Jawa*. <http://ppejawa.com/ekoregion/das-progo>
- SolekHUDIN, I., & Ang, K. C. (2012a). A DRBEM with a predictor-corrector scheme for steady infiltration from periodic channels with root-water uptake. *Engineering Analysis with Boundary Elements*, 36(8), 1199–1204. <https://doi.org/10.1016/j.enganabound.2012.02.013>
- SolekHUDIN, I., & Ang, K. C. (2012b). Suction Potential and Water Absorption from Periodic Channels in Different Types of Homogeneous Soils. *Electronic Journal of Boundary Elements*, 10(2), 42–55.
- SolekHUDIN, I., & Sumardi. (2017). A DRBEM for steady infiltration from periodic semi-circular channels with two different types of roots distribution. *AIP Conference Proceedings*, 1848(May). <https://doi.org/10.1063/1.4983947>
- SolekHUDIN, I., & Zulijanto, A. (2017). A Dual Reciprocity Boundary Element Method for Water Infiltration Problems in a Single Flat and Trapezoidal Irrigation Channels. *October*, 13–14.
- Vrugt, J. A., Hopmans, J. W., & Simunek, J. (2001). Calibration of a Two-Dimensional Root Water Uptake Model. *Social Science Society of America*, 65(4), 1027–1037.
- Warrick, A. W. (2002). *Soil Physics Companion* (A. W. Warrick (ed.)). CRC Press. <https://doi.org/10.1201/9781498710718-9>
- Zahroh, M., & SolekHUDIN, I. (2022). Root Water Uptake Process for Different Types of Soil in Unsteady Infiltration from Periodic Trapezoidal Channels. *Proceedings of the International Conference on Mathematics, Geometry, Statistics, and Computation (IC-MaGeStiC 2021)*, 96, 113–119. <https://doi.org/10.2991/acsr.k.220202.023>